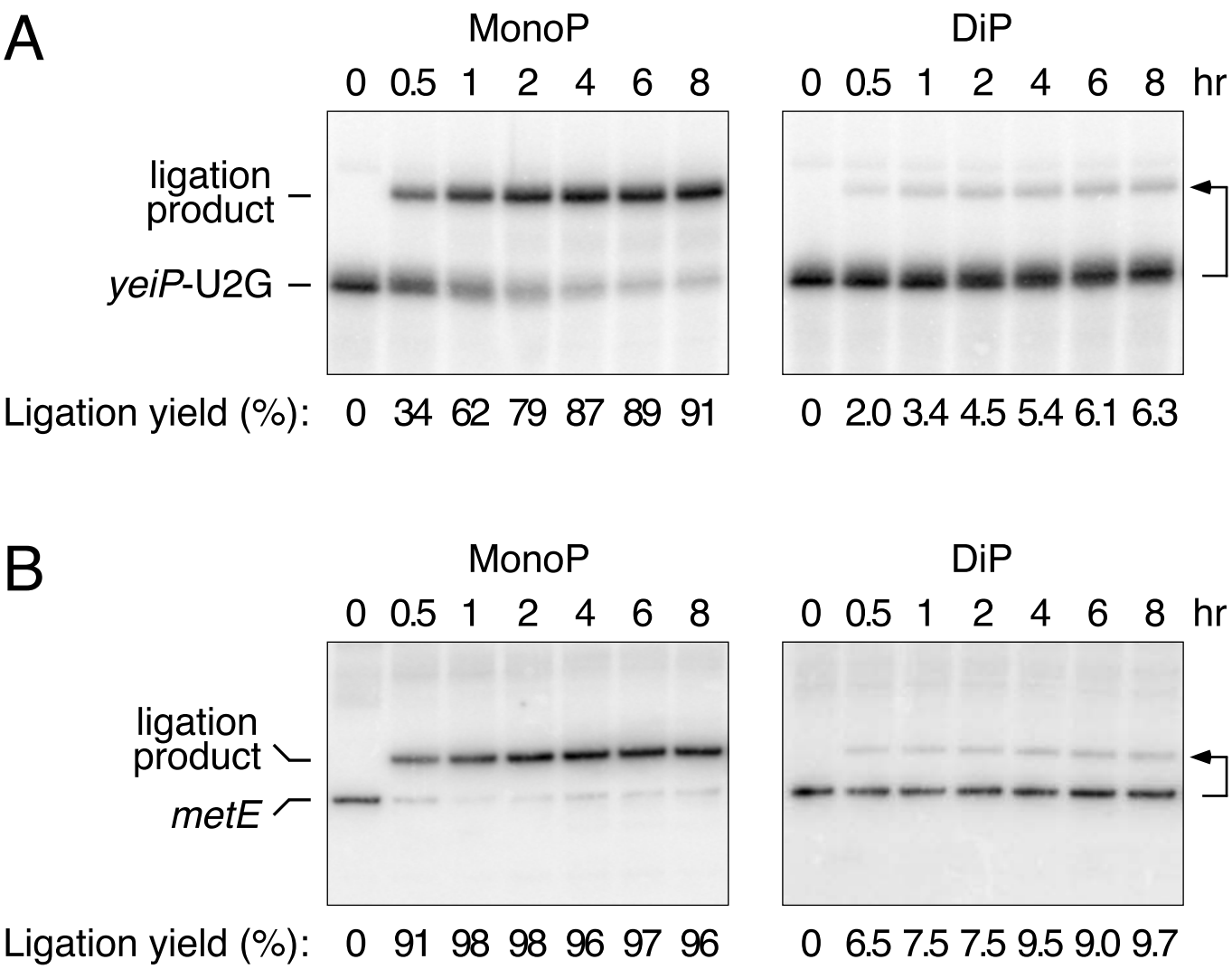

Figure S1. Relative reactivity of monophosphorylated and diphosphorylated RNA as PABLO substrates (related to Figures 3 and 4).

The splinted ligation of monophosphorylated (MonoP) and diphosphorylated (DiP) *in vitro* transcripts to a DNA oligonucleotide by T4 DNA ligase was monitored as a function of time in the presence of total *E. coli* RNA to simulate the analysis of an endogenous *E. coli* transcript by PABLO.

(A) *In vitro* transcribed *yeiP*-U2G RNA in the presence of total RNA from Δ*yeiP* cells.

(B) *In vitro* transcribed *metE* RNA in the presence of total RNA from Δ*metE* cells.

A bent arrow leads from the RNA substrate to its ligation product. In each case, the monophosphorylated substrate underwent ligation at least 13 times faster than its diphosphorylated counterpart.

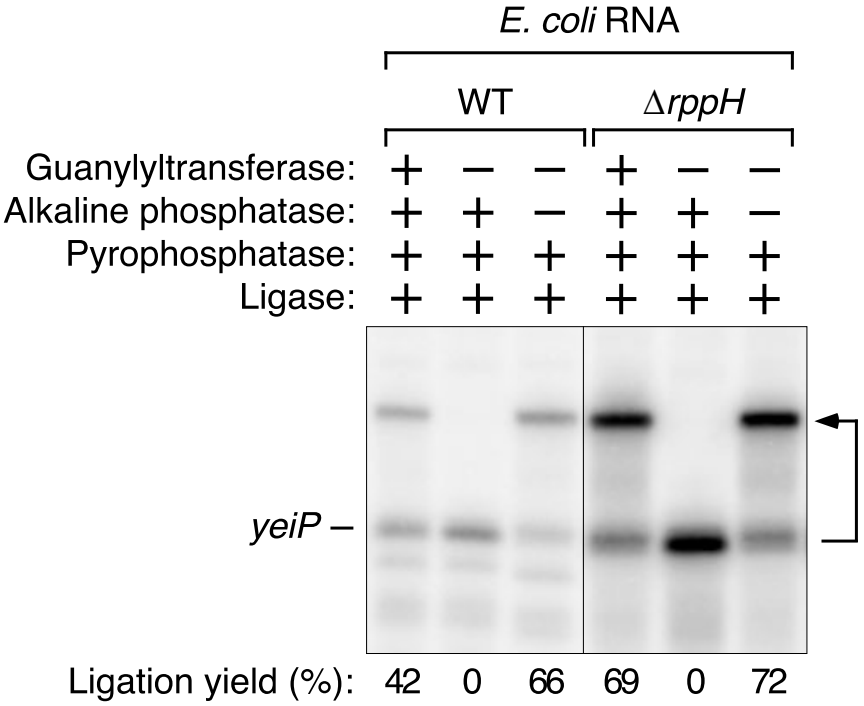

Figure S2. Detection of diphosphorylated *yeiP* mRNA in *E. coli* (related to Figure 3). The relative abundance of diphosphorylated *yeiP* mRNA was compared in wild-type (WT) and Δ*rppH* cells by PACO. As determined previously by PABLO (Richards et al., 2012), 43 ± 2% of the full-length *yeiP* transcript is monophosphorylated in wild-type cells, whereas almost none is monophosphorylated in Δ*rppH* cells. A bent arrow leads from the RNA substrate to its ligation product. A vertical line marks the location of superfluous lanes omitted from the image.

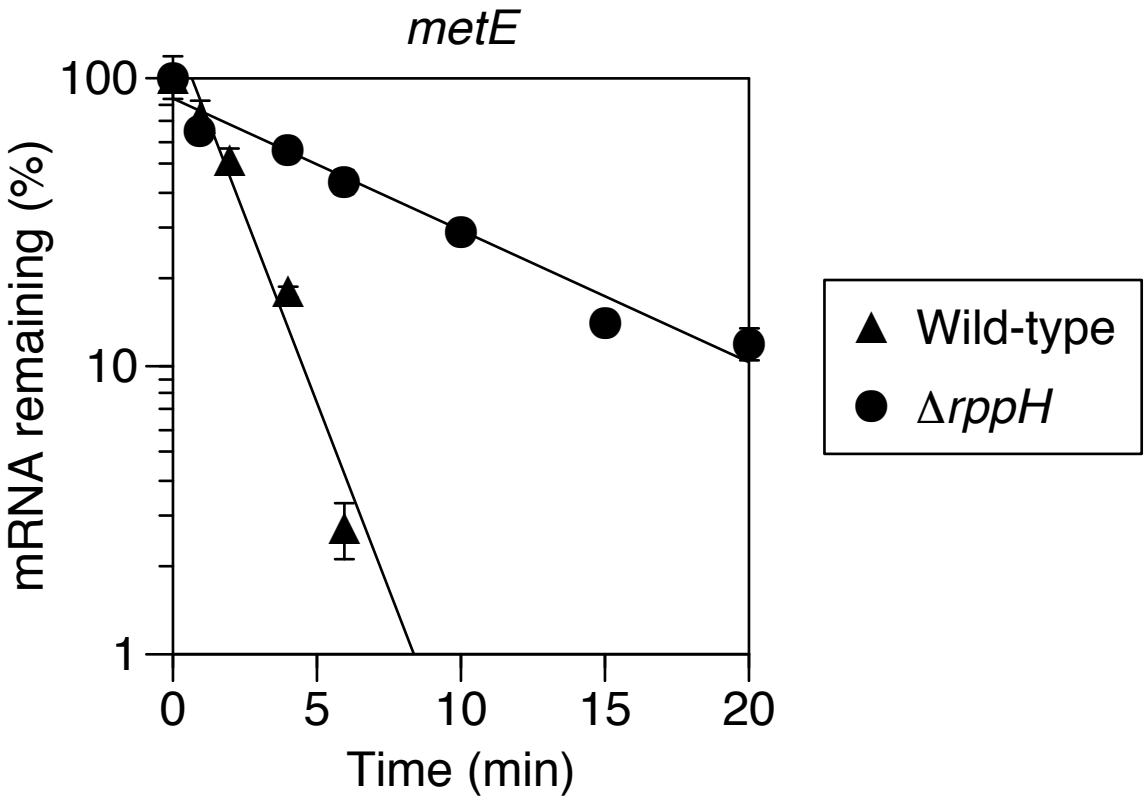

Figure S3. RppH-dependent decay of *metE* mRNA in *E. coli* (related to Figure 4). At time intervals after inhibiting transcription with rifampicin, total RNA was extracted from cultures of a pair of isogenic *E. coli* strains containing or lacking RppH, and the ratio of *metE* mRNA to 16S rRNA (a stable internal standard) in each sample was determined by quantitative RT-PCR and plotted semilogarithmically. Error bars represent standard deviations of multiple measurements. The observed half-life of *metE* mRNA increased from 1.2 ± 0.2 min in wild-type cells to 6.6 ± 0.5 min in Δ*rppH* cells.

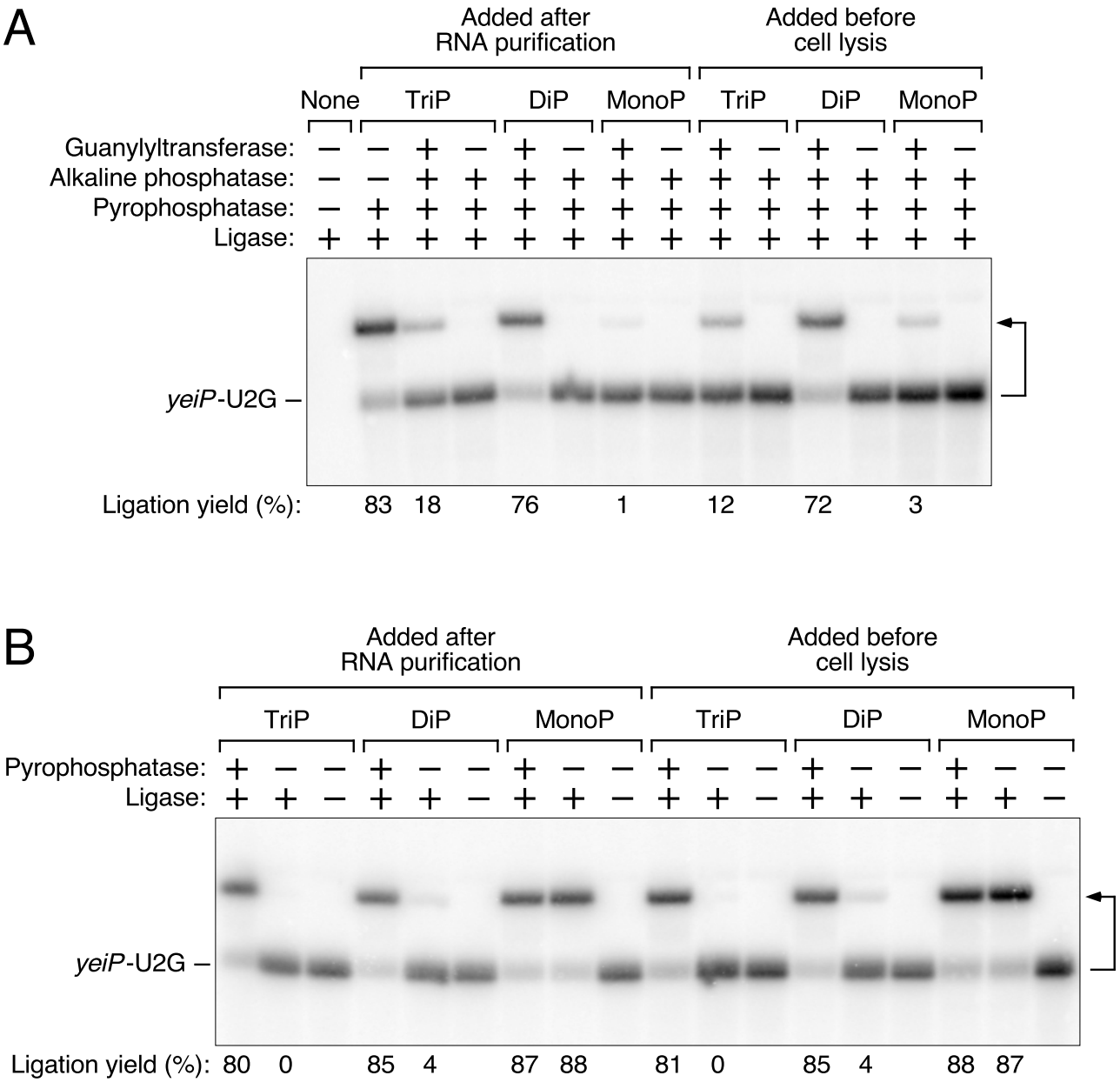

Figure S4. Unperturbed phosphorylation state of transcripts following RNA extraction from *E. coli* (related to Figure 3).

Fully triphosphorylated (TriP), diphosphorylated (DiP), or monophosphorylated (MonoP) *yeiP*-U2G RNA that had been synthesized by *in vitro* transcription (1.15 pmol) was added to intact *E. coli* cells from which the *yeiP* gene had been deleted (10 ml of a culture harvested at A_{650} = 0.3, pelleted, and resuspended), and total RNA was then extracted from those cells. Alteratively, the same *in vitro* transcripts (0.046 pmol) were added to total RNA (5 μg) following its extraction and purification from the cells. The phosphorylation state of the transcripts spiked in before or after the extraction procedure was then compared by (A) PACO and (B) PABLO. A bent arrow leads from the RNA substrate to its ligation product.

Table S1. Relative reactivity of diphosphorylated versus triphosphorylated dinucleotides (related to Figure 2).

	ppApG			**pppApG**		
Time (min)	DiP remaining (%)		Standard deviation	TriP remaining (%)		Standard deviation
0	100.00	±	0.00	100.00	±	0.00
1	39.69	±	0.74	89.21	±	0.98
2	2.56	±	0.28	80.04	±	1.29
3	0.19	±	0.07	71.67	±	1.69
4	0.00	±	0.00	64.46	±	2.15
6	0.00	±	0.00	52.37	±	2.28
8	0.00	±	0.00	42.02	±	2.32
10	0.00	±	0.00	34.13	±	2.28

	ppApA			**pppApA**		
Time (min)	DiP remaining (%)		Standard deviation	TriP remaining (%)		Standard deviation
0	100.00	±	0.00	100.00	±	0.00
1	48.98	±	0.01	93.65	±	1.08
2	9.80	±	2.06	88.13	±	1.62
3	0.60	±	0.19	83.01	±	2.16
4	0.12	±	0.00	78.19	±	2.67
6	0.00	±	0.00	69.67	±	3.49
8	0.00	±	0.00	62.11	±	4.10
10	0.00	±	0.00	55.28	±	4.58

	ppApU			**pppApU**		
Time (min)	DiP remaining (%)		Standard deviation	TriP remaining (%)		Standard deviation
0	100.00	±	0.00	100.00	±	0.00
1	54.69	±	0.02	96.76	±	0.83
2	24.65	±	1.85	93.95	±	0.96
3	9.27	±	1.47	91.44	±	1.22
4	3.52	±	0.81	88.97	±	1.17
6	0.00	±	0.00	84.38	±	1.50
8	0.00	±	0.00	80.05	±	1.47
10	0.00	±	0.00	75.96	±	1.61

	ppApC			**pppApC**		
Time (min)	DiP remaining (%)		Standard deviation	TriP remaining (%)		Standard deviation
0	100.00	±	0.00	100.00	±	0.00
1	63.81	±	7.86	97.49	±	0.69
2	38.69	±	10.79	95.70	±	0.97
3	22.62	±	10.35	93.98	±	1.18
4	12.71	±	8.17	92.71	±	1.17
6	4.15	±	3.81	89.58	±	1.51
8	1.40	±	1.56	86.94	±	1.70
10	0.47	±	0.59	84.28	±	1.80

Table S2. Measurements used to calculate the capping efficiencies of *yeiP*-U2G and *metE* standards synthesized by *in vitro* transcription (related to Figures 3 and 4).

	Measured values				5′ homogeneity	
	Y_{TS}	Y_{DS}	Y_{MS}	E_{LS}	D_S	M_S
yeiP-U2G	0.244 ± 0.067	0.692 ± 0.028	0.038 ± 0.021	0.802 ± 0.042	0.930	0.978
metE	0.142 ± 0.001	0.674 ± 0.014	0.027 ± 0.038	0.680 ± 0.020	0.974	0.975

Y_{TS}, Y_{DS}, and Y_{MS} are the fractional PACO ligation yields obtained for the triphosphorylated, diphosphorylated, and monophosphorylated standards, respectively. E_{LS} is the PABLO ligation efficiency of fully monophosphorylated RNA. The Y and E values correspond to the mean and standard deviation of two independent measurements. D_S and M_S are the calculated fractions of those standards that are diphosphorylated and monophosphorylated, respectively.

Table S3. Calculated capping efficiencies of *yeiP*-U2G and *metE* standards synthesized by *in vitro* transcription (related to Figures 3 and 4).

		Capping efficiencies		
		E_T	E_D	E_M
yeiP-U2G	Monte Carlo	$0.306^{+0.080}_{-0.089}$	$0.900^{+0.064}_{-0.057}$	$0.042^{+0.026}_{-0.029}$
	Direct calculation	0.304	0.905	0.042
metE	Monte Carlo	$0.209^{+0.006}_{-0.007}$	$1.014^{+0.035}_{-0.040}$	$0.035^{+0.057}_{-0.057}$
	Direct calculation	0.209	1.013	0.035

E_T, E_D, and E_M are the fractional capping efficiencies calculated for triphosphorylated, diphosphorylated, and monophosphorylated RNA, respectively, with 0 being no capping and 1 being complete capping. Each efficiency determined by Monte Carlo simulation corresponds to the peak of an asymmetric distribution, and the error range (±) corresponds to a confidence level of 68.3%, equivalent to one standard deviation. For comparison, the capping efficiencies were also calculated directly; these values agree well with the peak values obtained by Monte Carlo simulation, but only the simulation allowed error ranges to be determined. A minor discrepancy versus the theoretical maximum (1.000) resulted from the small mathematical correction factors that were used and is within the margin of error.

Table S4. Measurements used to calculate the phosphorylation state of *yeiP*-U2G and *metE* mRNA in *E. coli* (related to Figures 3 and 4).

	PACO				PABLO			
	Wild-type		Δ*rppH*		Wild-type		Δ*rppH*	
	Y_D	E_{LD}	Y_D	E_{LD}	Y_M	E_{LM}	Y_M	E_{LM}
yeiP-U2G	0.188 ± 0.004	0.570 ± 0.008	0.606 ± 0.004	0.627 ± 0.031	0.479 ± 0.012	0.655 ± 0.026	0.024 ± 0.0003	0.769 ± 0.008
metE	0.404 ± 0.038	0.700 ± 0.020	0.664 ± 0.015	0.666 ± 0.023	0.283 ± 0.010	0.899 ± 0.016	0.026 ± 0.004	0.904 ± 0.003

The phosphorylation state of *yeiP*-U2G and *metE* mRNA was compared in wild-type and Δ*rppH* *E. coli* cells by PACO and PABLO. Y_D and Y_M are the fractional PACO and PABLO ligation yields. E_{LD} and E_{LM} are the PABLO ligation efficiencies of fully monophosphorylated RNA. The values listed correspond to the mean and standard deviation of measurements on 2-3 biological replicates.

Table S5. Phosphorylation state of *yeiP*-U2G and *metE* mRNA in *E. coli* (related to Figures 3 and 4).

		Diphosphorylated		Monophosphorylated	
		Wild-type	Δ*rppH*	Wild-type	Δ*rppH*
yeiP-U2G	Monte Carlo	$^{+0.060}_{0.343}{}^{}_{-0.046}$	$^{+0.134}_{1.082}{}^{}_{-0.133}$	$^{+0.033}_{0.706}{}^{}_{-0.033}$	$^{+0.008}_{-0.032}{}^{}_{-0.008}$
	Direct calculation	0.352	1.088	0.707	– 0.032
metE	Monte Carlo	$^{+0.080}_{0.511}{}^{}_{-0.070}$	$^{+0.073}_{0.962}{}^{}_{-0.062}$	$^{+0.012}_{0.273}{}^{}_{-0.015}$	$^{+0.006}_{-0.051}{}^{}_{-0.008}$
	Direct calculation	0.516	0.968	0.271	– 0.051

The phosphorylation state of *yeiP*-U2G and *metE* mRNA was compared in wild-type and Δ*rppH E. coli* cells. Each fractional value determined by Monte Carlo simulation corresponds to the peak of an asymmetric distribution, and the error range (±) corresponds to a confidence level of 68.3%, equivalent to one standard deviation. For comparison, the fractional amounts of diphosphorylated and monophosphorylated *yeiP*-U2G and *metE* mRNA were also calculated directly; these values agree well with the peak values obtained by Monte Carlo simulation, but only the simulation allowed error ranges to be determined. Minor discrepancies versus the theoretical maximum (1.000) or minimum (0.000) resulted from the small mathematical correction factors that were used and are either within the margin of error or close to it. These small differences have no bearing on the conclusion that diphosphorylated mRNA is present and abundant in wild-type *E. coli*.

Table S6. Nucleotides used for *in vitro* transcription (related to Star Methods).

Nucleotide	Vendor	Catalog number	Nominal purity	Measured purity [1]
ATP	Roche	11140965001	≥ 98%	99.33% ATP 0.67% ADP
ADP	Sigma	A-5285	≥ 95%	99.50% ADP 0.50% AMP
AMP	Sigma	A-1752	≥ 99%	100% AMP
GTP	Roche	11140957001	≥ 98%	99.35% GTP 0.65% GDP
GDP	MP Biomedicals	02151213	~ 98%	97.68% GDP 2.32% GMP
GMP	Sigma	G-8377	≥ 99%	100% GMP
CTP	Roche	11140922001	≥ 98%	99.57% CTP 0.43% CDP
UTP	Roche	11140949001	≥ 98%	99.07% UTP 0.93% UDP

[1] As determined by anion-exchange chromatography.

Table S7. Oligonucleotides used in these studies (related to Star Methods).

Name	Sequence	Purpose
T7 metE fwd	AAAACAAATTAATACGACTCACTA TAGTAAACATCTGGACGGC	PCR primer for *metE in vitro* transcription (IVT) template
metE rev	AAAAGACCGGGTGGTATTACCACC CGGTTTGGATTTTACC	PCR primer for *metE* IVT template
T7 yeiP-U2G fwd	AAAAGAATTCCAAATTAATACGAC TCACTATTAGATTTTTGACATTTTC GACTACAGG	PCR primer for *yeiP*-U2G IVT template
yeiP rev	AAATTAAAAAAGGGACAGCCTGA GC	PCR primer for *yeiP*-U2G IVT template
yeiP 80 rev	GTAATTCAGTACCATACCTT	PCR primer for truncated *yeiP*-U2G IVT template [1]
yeiP 128 rev	AGTGGGCGACTGAATATC	PCR primer for truncated *yeiP*-U2G IVT template [2]
yeiP 444 rev	TTTCCAGATCAACGGTCTGCG	PCR primer for truncated *yeiP*-U2G IVT template [3]
DZmetE214	TCAGCTCGCGAGGCTAGCTACAAC GAGCAGGCCAAC	10-23 DNAzyme for cleaving *metE* [4]

DZyeiP69	GTAATTCAGTAGGCTAGCTACAACGACATACCTTTT	10-23 DNAzyme for cleaving *yeiP* and *yeiP*-U2G [5]
DZyeiP444	GGTTTCAACGAGGCTAGCTACAACGATTCCAGATCA	10-23 DNAzyme for cleaving *yeiP*-U2G prior to TLC [6]
DZEcIVTa54	ACCGAACGCAAGGCTAGCTACAACGAGCCGACCGCA	10-23 DNAzyme for cleaving EcIVTa [7]
X22	GAACAATATGAATGATAACTTG	X oligo for PACO/PABLO analysis of *yeiP*, *yeiP*-U2G, and EcIVTa
X32	AAAAAAAAAAGAACAATATGAATGATAACTTG	X oligo for PACO/PABLO analysis of *metE*
Y-metE	TAGCCGTCCAGATGTTTACCAAGTTATCATTCATATTGTTC	Y oligo for PACO/PABLO analysis of *metE*
Y-yeiP	AGTCGAAAATGTCAAAAATATCAAGTTATCATTCATATTGTTC	Y oligo for PACO/PABLO analysis of *yeiP*
Y-yeiP-U2G	AGTCGAAAATGTCAAAAATCTCAAGTTATCATTCATATTGTTC	Y oligo for PACO/PABLO analysis of *yeiP*-U2G
Y-EcIVTa	AGAAGAACAACAGAGAAAGATCAAGTTATCATTCATATTGTTC	Y oligo for PACO analysis of EcIVTa
metE probe	CAGGCCAACGCGAGGGAAACCGA	Northern blot probe for *metE*
yeiP probe	TTCGTTCGCTCTTGGCATCG	Northern blot probe for *yeiP* and *yeiP*-U2G
EcIVTa probe	GCCGACCGCACAGGGCAGGG	Northern blot probe for EcIVTa
qPCR metE fwd	ATGGTGCGTTGGCTGCGT	qPCR primer for *metE*
qPCR metE rev	CGAGGGAAACCGAGGGTGTG	qPCR primer for *metE*
qPCR 16S fwd	CTCTTGCCATCGGATGTGCCCA	qPCR primer for 16S rRNA
qPCR 16S rev	CCAGTGTGGCTGGTCATCCTCTCA	qPCR primer for 16S rRNA

[1] For synthesis of the first 80 nucleotides of *yeiP*-U2G RNA by *in vitro* transcription.

[2] For synthesis of the first 128 nucleotides of *yeiP*-U2G RNA by *in vitro* transcription.

[3] For synthesis of the first 444 nucleotides of *yeiP*-U2G RNA by *in vitro* transcription.

[4] Cuts 214 from the 5′ end of *metE*.

[5] Cuts 69 nucleotides from the 5′ end of *yeiP* and *yeiP*-U2G.

[6] Cuts 444 nucleotides from the 5′ end of *yeiP*-U2G.

[7] Cuts 54 nucleotides from the 5′ end of EcIVTa.